CARBON 66 (2014) 267–271

Available at www.sciencedirect.com

ScienceDirect

journal homepage: www.elsevier.com/locate/carbon

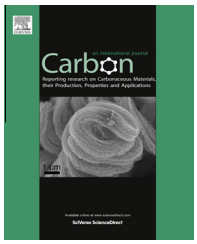

Graphene synthesis by C implantation into Cu foils

Jae Sung Lee [a], *Chan Wook Jang* [a], *Jong Min Kim* [a], *Dong Hee Shin* [a], *Sung Kim* [a], *Suk-Ho Choi* [a,*], *K. Belay* [b], *R.G. Elliman* [b]

[a] *Department of Applied Physics, College of Applied Science, Kyung Hee University, Yongin 446-701, Republic of Korea*

[b] *Department of Electronic Materials Engineering, Research School of Physics and Engineering, The Australian National University, Canberra, ACT 0200, Australia*

ARTICLE INFO

Article history:
Received 13 May 2013
Accepted 31 August 2013
Available online 7 September 2013

ABSTRACT

Cu foils of $2\times2\,cm^2$ have been implanted with 70 keV C^- ions to nominal fluences of $(2–10)\times10^{15}\,cm^{-2}$ at room temperature (RT) and subsequently annealed at 900–1100 °C for 15 min, before being cooled to RT to form graphene layers on the Cu surfaces. Analyses with Raman spectroscopy and atomic force microscopy demonstrate that a continuous film of bi-layer graphene (BG) is produced for implant fluences as low as $2\times10^{15}\,cm^{-2}$, much less than the carbon content of the BG films. This suggests that the implanted carbon facilitates the nucleation and growth of graphene, with additional carbon supplied by the Cu substrate (0.515 ppm carbon content). No graphene was observed on unimplanted Cu foils subjected to the same thermal treatment. This implantation method provides a novel technique for the selective growth of graphene on Cu surfaces.

1. Introduction

In recent years graphene has been studied as a novel nanomaterial for next-generation electronics and photonics due to its unique properties, which include: high carrier mobility [1], high thermal conductivity [2], tunable band gap [3], stretchable/visible transparency [4], and robust two-dimensionality [5]. The electronic and optical properties of graphene have been shown to depend strongly on its thickness, i.e., the number of graphene layers [1,3,6]. Chemical vapor deposition (CVD) has been recognized as a useful method to synthesize large-scale graphene layers with tunable thickness, one of the central issues in graphene-based electronics and photonics [4]. Controlled synthesis of single-layer graphene (SG) has been further improved by employing Cu instead of Ni as a catalyst in the CVD scheme [7]. Recently, physical methods, such as poly(methyl methacrylate) (PMMA) derivation on Cu film [8], deposition of amorphous carbon/Ni (or Co) bilayers [9], ion implantation of C into Ni films [10], and sputtering of graphite/Ni composite films [11], accompanied by annealing treatments, have been proposed to synthesize graphene layers. However, the maximum uniform area available from any of these techniques is far below what can be reached by CVD [12], one of the major reasons why the physical methods are not so competitive in graphene studies or industries as CVD at the moment. Even so, the physical methods have their unique advantages such as no use of chemical gases and precise control of C atoms (thus precise control of number of graphene layers).

The ion-implantation method has a particular advantage in that it does not require the metal catalyst to have high carbon solubility, but uniform, large-area synthesis of SG or BG by implantation of C into Ni films was not successful [10]. In this paper, we successfully synthesize uniform BG films over an area of $\sim2\times2\,cm^2$ by ion implantation of C into Cu foils and subsequent carefully-modified heat treatment. The synthesized graphene layers are optimized by controlling C fluence and annealing parameters of the C-implanted Cu foils based on the measurements by Raman spectroscopy and atomic force microscopy (AFM).

* *Corresponding author:* Fax: +82 31 204 8122.
E-mail address: sukho@khu.ac.kr (S.-H. Choi).

0008-6223/$ - see front matter
http://dx.doi.org/10.1016/j.carbon.2013.08.066

2. Experimental

Cu foils of $2 \times 2\,cm^2$ were implanted with 70 keV C^- ions to nominal fluences (ϕ_C) of (2, 4, 5, 8, and 10) $\times 10^{15}\,C\,cm^{-2}$ at room temperature (RT). The peak excess-C concentration for these implants was calculated from TRIM simulation to be in the range of 1.6×10^{20}–$8 \times 10^{20}\,C\,cm^{-3}$ (0.19–0.95 at.%) [13]. The C-implanted Cu foils were heated to the annealing temperature (T_A) under vacuum. After dwelling at T_A for 15 min, the samples were slowly cooled to RT at a rate of ~10 °C/min to form a graphene layer on the Cu foils. T_A was varied from 900 to 1100 °C. The graphene layer was easily transferred to a SiO_2/Si substrate by using a sacrificial PMMA layer as previously reported in the literature [4,14]. Briefly, after a PMMA layer had been spincoated onto the graphene layer/Cu foil, the Cu foil was etched away in an ammonium persulfate solution (1 M), thereby leaving the detached PMMA/graphene layer in a water bath. Then, the PMMA/graphene layer was transferred to a SiO_2/Si substrate, allowed to dry, and placed in an acetone bath to dissolve the PMMA support layer. After a rinse with water, the graphene layer was finally obtained on a SiO_2/Si substrate. In this work, two kinds of high-purity Cu foils (Alfa Aesar) were used: one of 0.515 ppm carbon content and the other free of carbon. No graphene was formed on Cu foils free of carbon by the same C-implantation and successive thermal treatment.

The synthesized graphene layers were characterized by using Raman spectroscopy and AFM. Micro (μ)-Raman measurements were carried out using a homebuilt scanning confocal microscope. The samples mounted on a scanning stage were excited by using the 532-nm line of a diode-pumped solid-state laser. The laser beam was focused on the sample surface through a microscope objective that could focus the laser excitation spot down to below 1 μm. The μ-Raman signal from the samples was spectrally dispersed by using a 50-cm spectrometer equipped with a charge coupled device (Andor DU401A-BV). A Raman mapping could finally be created by moving the sample under the microscope through the use of properly aligned stepping motors. The spatial resolution of the Raman mapping image was less than 1 μm. The thickness and morphology of the precipitated graphene were analyzed in the non-contact mode of an atomic force microscope (Park system, model XE-100).

3. Results and discussion

Annealing temperature, time, and environment are the important parameters affecting the synthesis of graphene layers. The annealing time was fixed at 15 min after it was systematically explored and optimized. For longer annealing times, the graphene formation and quality was severely degraded. Annealing was also performed under nitrogen or hydrogen, but was not so effective as under vacuum.

Fig. 1(a) shows Raman spectra of the Cu foils implanted with C^- ions to a fluence of $2 \times 10^{15}\,cm^{-2}$ before and after annealing. At $T_A = 1100$ °C, the Raman spectra of the C-implanted Cu foils exhibit the most intense *G* and 2*D* peaks at ~1580 and ~2700 cm^{-1}, respectively, uniquely characteristic of graphene films [15–17]. In contrast, the as-implanted films

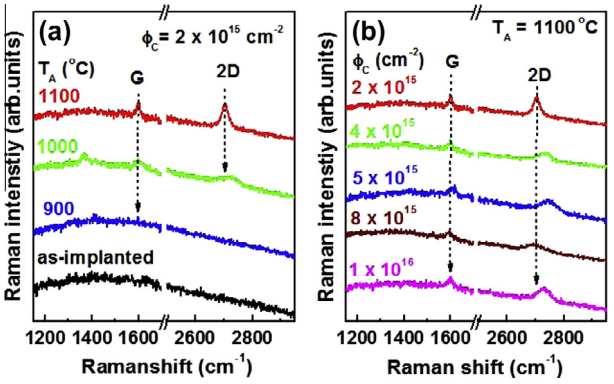

Fig. 1 – Raman spectra of C-implanted Cu foils (a) for various annealing temperatures at a fixed fluence of $2 \times 10^{15}\,cm^{-2}$ and (b) for various fluences at a fixed annealing temperature of 1100 °C. (A colour version of this figure can be viewed online)

exhibit no Raman peaks over the full measurement range. The intensities and shapes of the Raman peaks strongly depend on the fluence as well as on the annealing temperature, as shown in Fig. 1(b). The *G* and 2*D* peaks are most distinctive and intense under a preparation condition of $\phi_C = 2 \times 10^{15}\,cm^{-2}$ and $T_A = 1100$ °C.

The Raman spectra were also detected after the graphene layers were transferred to SiO_2/Si substrates. Fig. 2(a) and (c) show the T_A- or ϕ_C-dependence of the Raman spectra, respectively, showing clear features for *D* (~1350 cm^{-1}), *G*, and 2*D* peaks. The Raman intensity ratios of the *G* to the 2*D* peaks (determined by the number of stacked graphene layers) and the *D* to *G* peaks (measure of disorder), defined as $\langle G/2D \rangle$ and $\langle D/G \rangle$, were calculated and are plotted as functions of T_A and ϕ_C in Fig. 2(b) and (d), respectively. A typical sample with $\phi_C = 2 \times 10^{15}\,cm^{-2}$ and $T_A = 1100$ °C has a $\langle G/2D \rangle$ value of ~0.8, suggesting the strong interlayer coupling typical of BG [14]. The thickness and disorder of the graphene sheets on SiO_2/Si show monotonic correlations with T_A and ϕ_C, as shown in Fig. 2(b) and (d). As T_A increases for the same supply of C atoms at a fixed ϕ_C, the precipitated graphene layers are expected to become more stoichiometric, thereby reducing their thickness and disorder, consistent with the results in Fig. 2(b). When more C atoms (higher ϕ_C) are supplied at a fixed T_A, the film is degraded by the excess carbon, as shown in Fig. 2(d). This Raman analysis reveals an optimum fluence (=$2 \times 10^{15}\,cm^{-2}$) and annealing temperature (= 1100 °C) for the synthesis of fewest-layer-number and best-quality graphene.

Spatial intensity mapping of Raman peaks of a typical sample with $\phi_C = 2 \times 10^{15}\,cm^{-2}$ and $T_A = 1100$ °C were taken at 1 μm steps across the whole area of $2 \times 2\,cm^2$ to check the spatial homogeneity of the graphene layers, as shown for a typical area of $100 \times 100\,\mu m^2$ in Fig. 3. The overall uniform frequency and intensity of the *G* peak associated with sp^2 carbon bond stretching [15–17] suggest that the graphene film is of high quality over full area of the sample. The mapping images of the 2*D* peak, sensitive to graphene interlayer interactions [15–17], further indicate uniform thickness of the graphene sheets. These results suggest that the areal uniformity of

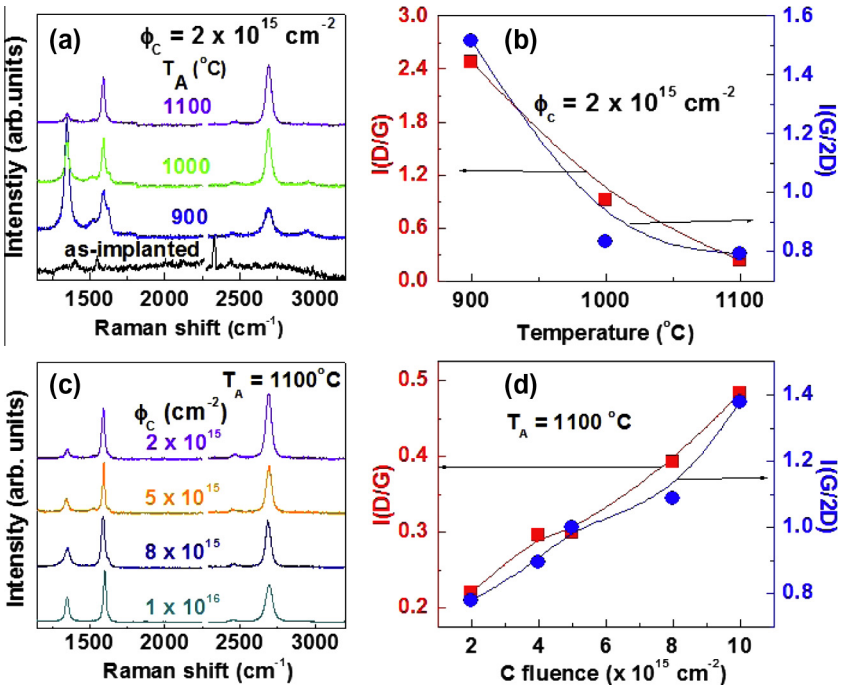

Fig. 2 – Raman spectra of graphene layers (a) for various annealing temperatures at a fixed fluence of 2×10^{15} cm^{-2} and (c) for various fluences at a fixed annealing temperature of 1100 °C. The Raman spectrum of an as-implanted sample ($\phi_C = 2 \times 10^{15}$ cm^{-2}) is also shown in Fig. 2(a) for comparison. The ⟨D/G⟩ and ⟨G/2D⟩ intensity ratios of graphene layers (b) as functions of annealing temperature at a fixed fluence of 2×10^{15} cm^{-2} and (d) as functions of fluence at a fixed annealing temperature of 1100 °C. (A colour version of this figure can be viewed online)

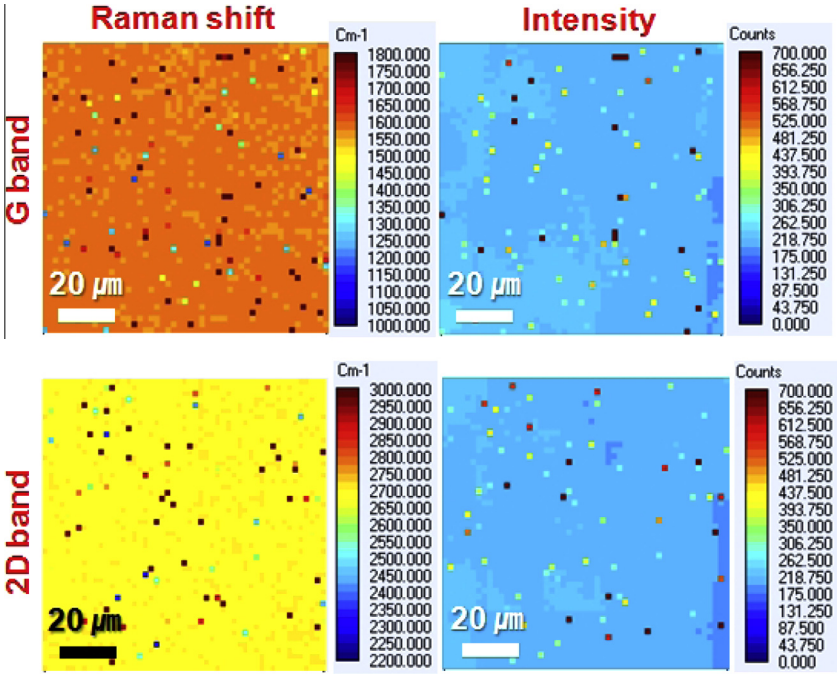

Fig. 3 – Spatial frequency and intensity mappings of Raman G and 2D bands for a typical sample with $\phi_C = 2 \times 10^{15}$ cm^{-2} and T_A = 1100 °C. (A colour version of this figure can be viewed online)

the graphene synthesized by ion implantation of C is greatly improved compared to the previous report [10].

AFM was used to measure the thickness of the precipitated graphene after it had been transferred on SiO_2. Fig. 4(a) shows an AFM topographic image of a typical sample with

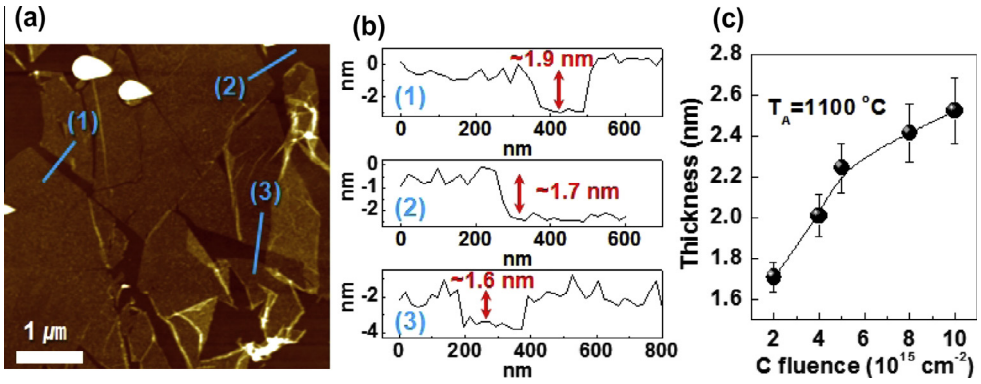

Fig. 4 – (a) AFM topographic image of a typical sample with $\phi_C = 2 \times 10^{15}$ cm^{-2} and $T_A = 1100$ °C. (b) AFM height profiles along the three different solid blue lines on the graphene sheet of (a). (c) Average thickness of graphene layers estimated by AFM height profiles as a function of fluence at a fixed annealing temperature = 1100 °C. (A colour version of this figure can be viewed online)

$\phi_C = 2 \times 10^{15}$ cm^{-2} and $T_A = 1100$ °C. The height profiles along the three different solid blue lines on the graphene sheet, as indicated in Fig. 4(a), show that the thickness of the graphene ranges from ~1.6 to ~1.9 nm, respectively, as shown in Fig. 4(b). Although the thickness of freestanding SG is fundamentally known to be 0.34 nm, practical AFM measurements always lead to higher values (0.6~1.6 nm) for the thickness of SG on SiO_2 due to the weak interactions/presence of ambient species (nitrogen, oxygen, or water) between the SiO_2 and the SG [6,18,19]. This effect is even higher for few-layer graphene due to the greatly-enhanced roughness caused by the increased layer number and the interlayer spacing [18,19]. Thus, the AFM measurements are consistent with BG [6,18], and with the Raman results in Fig. 2. The average thickness of graphene layers estimated by the AFM height profiles monotonically increases with increasing ϕ_C at a fixed $T_A = 1100$ °C, as shown in Fig. 4(c), also consistent with the Raman results in Fig. 2(d).

The synthesis of continuous BG films for samples implanted to a fluence of 2×10^{15} C cm^{-2} is intriguing as the total implant fluence represents only ~0.5 monolayers of graphene, much less than that required to produce a continuous BG film. This suggests that the implanted carbon facilitates the nucleation and growth of graphene, with additional carbon being supplied from a secondary C source, most likely the Cu foils (0.515 ppm carbon content). The growth mechanism is likely similar to that of the dissolution-precipitation method [4,9,20], in which carbon segregates on the catalyst surface due to a reduction in the bulk-carbon solubility during cooling but with an additional near-surface carbon source provided by the C implantation. It appears that the implanted carbon initiates the nucleation and growth of graphene and that this acts as a sink for additional carbon present in the Cu foil. This is consistent with the observation that no graphene was formed on unimplanted samples annealed under the same conditions. Importantly, the number and the quality of graphene layers were easily controlled by varying the implant fluence and annealing temperature.

4. Conclusion

Cu foils of 2×2 cm^2 were implanted with 70 keV C^- ions by varying ϕ_C from 2×10^{15} to 1×10^{16} cm^{-2} at RT and subsequently annealed at $T_A = 900$–1100 °C under vacuum for 15 min to form graphene layers on Cu surfaces. As analyzed by Raman spectroscopy and AFM, the BG defect-minimized and spatially uniform over whole area of $\sim 2 \times 2$ cm^2 was formed at $\phi_C = 2 \times 10^{15}$ cm^{-2} and $T_A = 1100$ °C. A possible synthesis mechanism was discussed to explain the ϕ_C- and T_A-dependent growth behaviors of the graphene layers. This approach provides an advantage in that the number of layers can be simply tuned by varying fluence at a fixed annealing temperature of 1100 °C, promising for reliably-controlled physical synthesis of graphene on a large scale.

Acknowledgments

This work was supported by Basic Science Research Program through the National Research Foundation of Korea (NRF) funded by the Ministry of Science, ICT & Future Planning (No. 2011-0017373).

REFERENCES

[1] Geim AK, Novoselov KS. The rise of graphene. Nature Mater 2007;6:183–91.
[2] Balandin AA, Ghosh S, Bao W, Calizo I, Teweldebrhan D, Miao F, et al. Superior thermal conductivity of single-layer graphene. Nano Lett 2008;8:902–7.
[3] Zhang Y, Tang TT, Girit C, Hao Z, Martin MC, Zettl A, et al. Direct observation of a widely tunable bandgap in bilayer graphene. Nature 2009;459:820–3.
[4] Kim KS, Zhao Y, Jang H, Lee SY, Kim JM, Kim KS, et al. Large-scale pattern growth of graphene films for stretchable transparent electrodes. Nature 2009;457:706–10.

[5] Lee C, Wei X, Kysar JW, Hone J. Measurement of the elastic properties and intrinsic strength of monolayer graphene. Science 2008;321:385–8.
[6] Novoselov KS, Geim AK, Morozov SV, Jiang D, Zhang Y, Dubonos SV, et al. Electric field effect in atomically thin carbon films. Science 2004;306:666–9.
[7] Li X, Cai W, An J, Kim S, Nah J, Yang D, et al. Large-area synthesis of high-quality and uniform graphene films on copper foils. Science 2009;324:1312–4.
[8] Sun Z, Yan Z, Yao J, Beitler E, Zhu Y, Tour JM. Growth of graphene from solid carbon sources. Nature 2010;468:549–52.
[9] Zheng M, Takei K, Hsia B, Fang H, Zhang X, Ferralis N, et al. Metal-catalyzed crystallization of amorphous carbon to graphene. Appl Phys Lett 2010;96:063110. 1-3.
[10] Garaj S, Hubbard W, Golovchenko JA. Graphene synthesis by ion implantation. Appl Phys Lett 2010;97:183103. 1-3.
[11] Shin DH, Yang SB, Shin DY, Kim CO, Kim S, Choi SH, et al. Graphene synthesis from graphite/Ni composite films grown by sputtering. J Korean Phys Soc 2012;61:563–7.
[12] Bae S, Kim H, Lee Y, Xu X, Park JS, Zheng Y, et al. Roll-to-roll production of 30-inch graphene films for transparent electrodes. Nature Nanotech 2010;5:574.
[13] Biersack P, Haggmark LG. A Monte Carlo computer program for the transport of energetic ions in amorphous targets. Nucl Instrum Methods Phys Res B 1980;174:257–69.
[14] Yu Q, Lian J, Siriponglert S, Li H, Chen YP, Pei SS. Graphene segregated on Ni surfaces and transferred to insulators. Appl Phys Lett 2007;93:113103. 1-3.
[15] Gupta A, Chen G, Joshi P, Tadigadapa S, Eklund PC. Raman scattering from high-frequency phonons in supported n-graphene layer films. Nano Lett 2006;6:2667–73.
[16] Ferrari AC, Meyer JC, Scardaci V, Casiraghi C, Lazzeri M, Mauri F, et al. Raman spectrum of graphene and graphene layers. Phys Rev Lett 2006;97:187401. 1-4.
[17] Graf D, Molitor F, Ensslin K, Stampfer C, Jungen A, Hierold C, et al. Spatially resolved Raman spectroscopy. Nano Lett 2007;7:238–42.
[18] Giannazzo F, Sonde S, Raineri V, Patanè G, Compagnini G, Aliotta F, et al. Optical, morphological and spectroscopic characterization of graphene on SiO_2. Phys Status Solidi C 2010;7:1251–5.
[19] Wu ZS, Ren W, Gao L, Liu B, Jiang C, Cheng HH. Synthesis of high-quality graphene with a pre-determined number of layers. Carbon 2009;47:493–9.
[20] Reina A, Jia X, Ho J, Nezich D, Son H, Bulovic V, et al. Large area, few-layer graphene films on arbitrary substrates by chemical vapor deposition. Nano Lett 2009;9:30–5.